ESTIMATING EXTREME WAVE DESIGN CRITERIA INCORPORATING DIRECTIONALITY

Kevin Ewans
Shell International Exploration and Production
P.O. Box 60, 2280 AB Rijswijk, The Netherlands.
e-mail: kevin.ewans@shell.com

Philip Jonathan
Shell Research Limited
P.O. Box 1, Chester, United Kingdom.
e-mail: philip.jonathan@shell.com

1. INTRODUCTION

Environmental design criteria for offshore facilities have inherent uncertainties. These uncertainties are a function of climate variability in time, space and storm peak direction and track. The quality of estimation of design criteria is further dependent on data sample size.

In a previous study (Elsinghorst et al., 1998), application of Generalised Pareto modelling to estimation of North Sea storm severity is reported for storms with return periods of 100 to 500 years based on NESS hindcast data. The study consisted of the following elements. The tail distribution of storm severity was modelled and magnitudes of extreme events with long return periods estimated. Uncertainty of estimates was quantified using a bootstrapping approach. Finally, bias and coverage for estimates of uncertainty were quantified by simulation study.

Site averaging can be used to increase the sample size for modelling, and to account for randomness of storm track, in hurricane-dominated regions (Forristall et al., 1991). However, hurricane data from even quite largely separated locations are highly correlated. Thus careful quantification of uncertainty of parameter estimates and extreme quantiles is necessary, accommodating this dependency structure. Jonathan and Ewans (2006) adopt a bootstrapping approach to calculate interval estimates for GPD model parameters and extreme quantiles to account for spatial dependence of extremes when site-averaging is used.

The inherent directionality of metocean data is the subject of this paper. In most regions, but particularly hurricane-dominated regions (e.g. Gulf of Mexico), and in regions where extra-tropical storms prevail (e.g. Northern North Sea), the extremal properties of storms are also highly dependent on storm peak direction.

Accordingly, sea state design criteria for offshore facilities are frequently provided by direction, in order to optimise engineering facilities for the directional environment. For example, it is typical for return-period values of the significant wave height to be specified for each of eight 45° sectors in addition to the omni-directional case. However, debate continues (e.g. Forristall, 2004) on how these should be derived in a consistent way. This is addressed in this paper and a method for developing criteria for a directional environment is proposed.

Theory and application of extreme value modelling is summarised, for example, by Kotz and Nadarajah (2000) and Reiss and Thomas (2001). The former authors provide an interesting overview of applications including those of Coles, Tawn and co-workers. For example, Coles and Walshaw (1994) model extremal properties of wind speeds as a function of their direction, accounting during fitting for angular dependency structure, by inflating standard errors for parameter estimates. Robinson and Tawn (1997) apply a Fourier model to characterise the extremal behaviour of sea currents. Coles and Powell (1996) discuss a Bayesian approach to extreme value estimation using data from multiple locations. Coles and Casson (1998), Casson and Coles (1999) present spatial models for extremes. Coles and Tawn (1996, 2005) discuss the estimation of predictive distributions (for quantities such as H_{S100}), which incorporate uncertainties in model parameters.

The paper is arranged as follows. In section 2, we introduce the GOMOS hindcast data motivating the investigation, illustrating some key features. In section 3, an outline of the Generalised Pareto Distribution (GPD) used to characterise the extreme value behaviour of the data is given. We also present a directional model for the parameters of the GPD distribution, and outline the application of maximum likelihood to estimate the paremeters of the directional model, and their uncertainties. Further detail of the maximum likelihood estimation is given as in Appendix A. We then apply the directional model to the GOMOS data. In section 4, we extend the model to estimate the distributional properties of the 100-year significant wave height H_{S100} and illustrate our findings using GOMOS. In section 5, we discuss the estimation of design criteria in the presence of directional dependence, and evaluate implications for designs at GOMOS. In section 6, we summarise findings and make suggestions and recommendations for future studies.

2. DATA

The data examined are significant wave height, H_S, values from the proprietary GOMOS Gulf of Mexico hindcast Study (Oceanweather, 2005), for the period September 1900 to September 2005 inclusive, at 30-minute intervals. For a typical Gulf of Mexico location, we selected 120 grid points arranged on a 15 x 8 rectangular lattice with spacing with 0.125˚ (14 km). For each storm period for each grid point, we isolated storm peak significant wave height, H_S^{sp}, for modelling purposes, together with the corresponding wave direction at storm peak H_S, henceforth referred to as storm peak direction.

Figure 1 shows H_S^{sp} as a function of storm peak direction for all locations. Storm peak direction is defined clockwise from the North. It is apparent from the figure that storms are more frequent in the directional sector $[0,180]$, which also contains the highest values of H_S^{sp}. Storms are relatively infrequent in $[270,360]$. Inset in Figure 1 is the corresponding data for a single central location. Figure 2 illustrates the strength of dependence between values of H_S^{sp} at diagonally opposite grid locations, and also the dependence between storm peak directions at those locations.

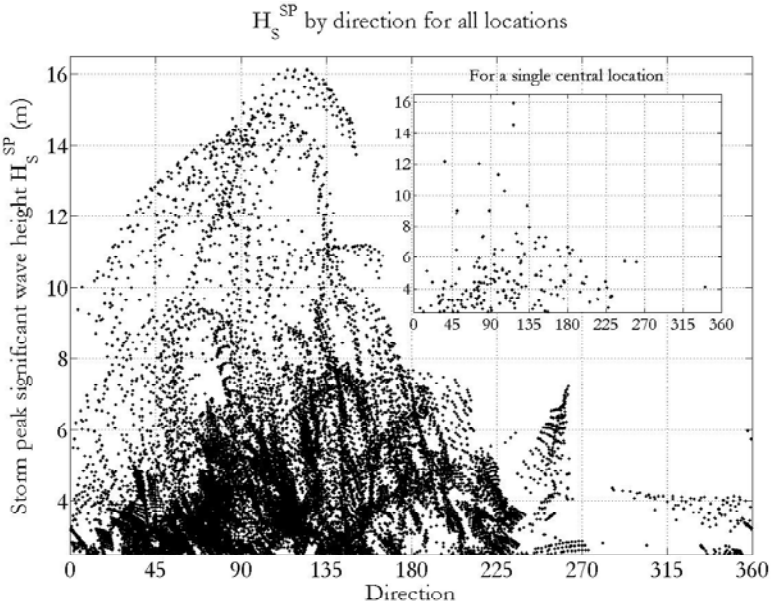

Figure 1. Storm peak significant wave height H_S^{sp} above a threshold of 2.5m as a function of direction for all locations. Inset: H_S^{sp} by direction for a single central location.

We note at this point that storm events do not correspond to a single wave direction only. Indeed, 30-minute sea states for a given storm event extend over a wide range of wave directions in general. Nevertheless, we characterise a storm in terms of its storm peak significant wave height, H_S^{sp} and storm peak direction, for the purposes of extreme value analysis in the peak over threshold sense. However, in estimating directional design criteria, we also account for the influence of storms over their full range of sea states and wave directions, as will be described further in section 4 below.

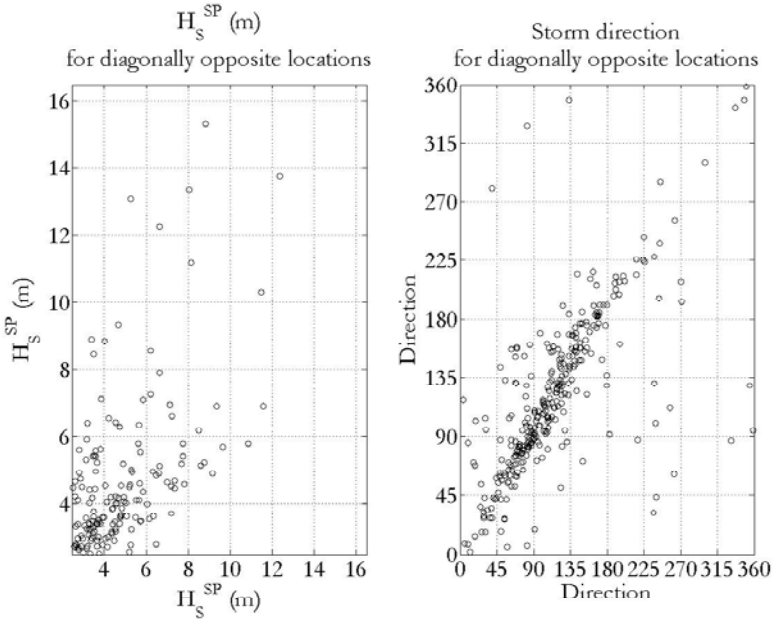

Figure 2. Scatter plot to illustrate dependence of storm peak significant wave height H_S^{SP} and storm peak direction for diagonally opposite locations, approximately 130 km apart.

3. MODELLING EXTREMAL PROPERTIES INCORPORATING DIRECTIONALITY

Suppose that we have data for storm peak significant wave heights $\{X_i\}_{i=1}^n$ and corresponding storm peak directions $\{\theta_i\}_{i=1}^n$ for a set of n storm events $\{E_i\}_{i=1}^n$ occurring in some period P_0. We assume, for any storm, that the distribution of extreme wave heights above a certain threshold u can be described using the Generalised Pareto Distribution (GPD) with cumulative distribution function $F_{X_i|\theta_i,u}$ given by:

$$F_{X_i|\theta_i,u}(x) = P\left(X_i \le x \mid \theta_i, u\right) = 1 - \left(1 + \frac{\gamma(\theta_i)}{\sigma(\theta_i)}(x-u)\right)_+^{-\frac{1}{\gamma(\theta_i)}} \quad \text{for } x > u, \sigma > 0$$

where $\gamma(\theta_i)$ is the shape parameter or tail index, $\sigma(\theta_i)$ is the scale, and u (assumed constant with respect to direction) is the threshold. We note that shape and scale parameters are functions of storm peak direction. The corresponding density function is:

$$f_{X_i|\theta_i,u}(x;\gamma,\sigma) = \frac{1}{\sigma(\theta_i)}\left(1 + \frac{\gamma(\theta_i)}{\sigma(\theta_i)}(x-u)\right)^{-\frac{1}{\gamma(\theta_i)}-1} \quad \text{for } x > u, \sigma > 0$$

Pickands (1975) has shown, for sufficiently high threshold u, that the GPD provides a good representation for any function $F_{X_i|\theta_i,u}$, in the sense that:

$$\lim_{u \to x_o} \sup_{0 < x < x_o - u} \left| F_{X_i|\theta_i,u} - F_{GPD}(x;\gamma,\sigma) \right| = 0$$

where x_o is the upper tail point of $F_{X_i|\theta_i,u}$.

In common with other authors (e.g. Robinson and Tawn, 1997), since we expect the extreme value parameters γ and σ to vary smoothly with direction, we characterise their directional dependence using a Fourier series expansion $\sum_{k=0}^{p} \sum_{b=1}^{2} A_{abk} t_b(k\theta)$, where $t_1 = \cos$, $t_2 = \sin$, with $a = 1$ for γ, and $a = 2$ for σ. We set $A_{a20} = 0$, $a = 1,2$ since this parameter is indeterminate. p is the order of the Fourier model, $p = 0$ corresponding to a constant model. Thus, for example, we refer to the cases $p = 1$ and $p = 3$ as first- and third- order directional models respectively.

We estimate the parameters A_{abk}, $a = 1,2$, $b = 1,2$, $k = 1,2,\ldots,p$ using maximum likelihood estimation. The likelihood of a data sample is given by:

$$L\left(\{A_{abk}\};\{X_i\}_{i=1}^{n}\right) = \prod_{i=1}^{n} \frac{1}{\sigma(\theta_i)} \left(1 + \frac{\gamma(\theta_i)}{\sigma(\theta_i)}(X_i - u)\right)^{-\frac{1}{\gamma(\theta_i)}-1}$$

The negative log likelihood is given by:

$$l\left(\{A_{abk}\};\{X_i\}_{i=1}^{n}\right) = \sum_{i=1}^{n} l_i \qquad \text{where} \qquad l_i = \log\sigma(\theta_i) + \left(\frac{1}{\gamma(\theta_i)} + 1\right) \log\left(1 + \frac{\gamma(\theta_i)}{\sigma(\theta_i)}(X_i - u)\right) \qquad \text{for}$$

$i = 1,2,\ldots,n$.

Maximum likelihood (or minimum negative log likelihood) estimates are found by setting the partial derivatives of l with respect to the parameter set A_{abk}, $a = 1,2$, $b = 1,2$, $k = 1,2,\ldots,p$ equal to 0. For further details, see Appendix A. Similarly, the asymptotic covariance matrix of the parameter estimates is given by the inverse I^{-1} of the information matrix, $I = E_X\left(\left\{\frac{\partial^2 l}{\partial A_{abk}^2}\right\}\right)$. Asymptotic variances for functions of the parameters, e.g. H_{S100}, can be derived also from I^{-1} (see Appendix A). Asymptotic variances for parameter estimates facilitate a studentised bootstrapping resampling analysis (see, e.g. Jonathan and Ewans, 2006), which allows reliable interval estimates for parameters to be calculated.

The first-order directional model, when applied to the GOMOS data for all 120 locations, yields the functional relationships:

$$\gamma = -0.13 + 0.24\cos(\theta) + 0.24\sin(\theta)$$

$$\sigma = 1.97 - 1.04\cos(\theta) + 0.14\sin(\theta)$$

for γ and σ with direction, illustrated in Figure 3 with the H_S^{SP} data for comparison. Figure 4 compares the functional forms of γ and σ with storm peak direction for first-, second- and third-order models. Also given in Figure 4 are estimates for γ and σ found independently using data from consecutive directional sectors of width 45°. It is clear that the directional model produces smooth estimates that are broadly consistent with the independent fits. From Figure 4 we judge that the first-order model adequately characterises the variability of extreme value parameters with storm peak direction, whilst noting that more formal model selection procedures might be useful in practice. Clearly the most appropriate model order depends on the application; higher order models would be necessary for locations with more complex directional dependence.

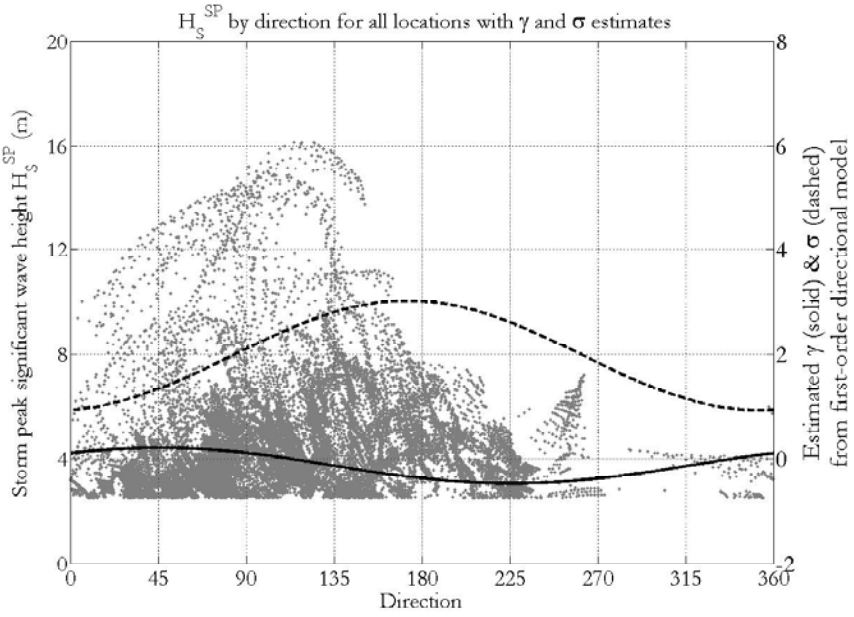

Figure 3. First-order directional model applied to GOMOS data for all locations. Figure shows H_S^{SP} and estimated γ and σ as a function of storm peak direction.

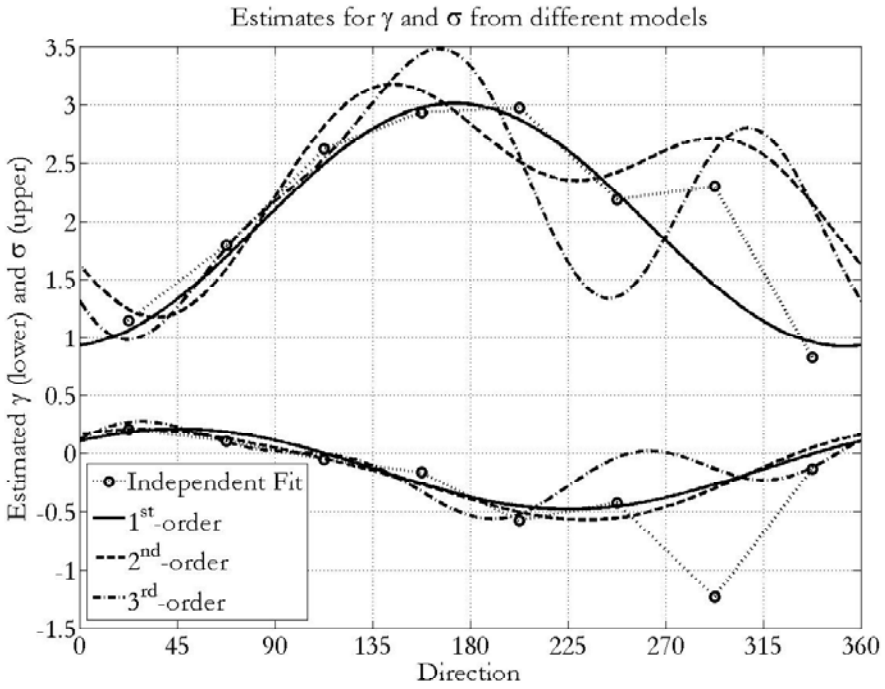

Figure 4. First-, second- and third-order directional models for GOMOS data for all locations. Also shown are independent estimates for γ and σ calculated using data from consecutive directional sectors of width 45°. The corresponding zero-order (constant) estimates for γ and σ are respectively -0.019 and 2.22.

Given the Fourier series form $\sum_{k=0}^{p}\sum_{b=1}^{2} A_{abk}t_b(k\theta)$ with $a=1$ for γ, and $a=2$ for σ, we can write $\frac{\partial l}{\partial A_{abk}} = \sum_{i=1}^{n} U_{ai}t_b(k\theta_i)$, $a=1,2$, $b=1,2$, $k=0,1,\ldots,p$ where $U_{ai}=\frac{\partial l_i}{\partial\gamma}$ for $a=1$, and $\frac{\partial l_i}{\partial\sigma}$ for $a=2$, recalling that $A_{a20}\triangleq 0$. Further, as outlined in Appendix A, $E_X\left[\frac{\partial^2 l}{\partial A_{abk}\partial A_{\alpha\beta\kappa}}\right] = \sum_{i=1}^{n}\frac{B_{a\alpha i}}{C_i}t_b(k\theta_i)t_\beta(\kappa\theta_i)$ $\forall a,b,k,\alpha,\beta,\kappa$. Thus, the information matrix $I = E_X\left[\left\{\frac{\partial^2 l}{\partial A_{abk}\partial A_{\alpha\beta\kappa}}\right\}\right]$ can be estimated for any sample of data. In particular, if we assume first-order models for each of γ and σ, I will be a 6×6 matrix. From the inverse of the information matrix, we obtain estimates for the asymptotic variances of the parameters $\{A_{abk}\}_{a=1,b=1,k=0}^{2,2,p}$. Similarly, asymptotic variances for γ, σ can be estimated given knowledge of the partial derivatives of the γ, σ with respect to the A_{abk}. We refer the reader to Appendix A for further discussion. Using these expressions, asymptotic 95% confidence bands for γ and σ with direction are given in Figure 5. The lines representing the asymptotic limits are barely distinguishable from those representing the maximum likelihood estimates.

Due to the spatial dependence structure of the data, it has been shown that bootstrapping can be used to estimate more realistic interval estimates for model parameters. Bootstrapping is a standard approach in statistics and involves estimating parameter uncertainty by resampling the original data sample (e.g. Hall, 1988, Efron and Tibshirani, 1993, Davison and Hinkley, 1997). Coles and Simiu (2003) discuss a number of difficulties in applying bootstrapping for estimation of uncertainties in extreme value analysis, including the tendency to underestimate extreme quantiles. Nevertheless, they conclude that bootstrapping, carefully applied, can be used reliably to give realistic estimates for parameter uncertainties. Heffernan and Tawn (2004) report a conditional approach for extreme value analysis applicable to higher dimensional problems, also incorporating bootstrapping, in which dependence structure is characterised using rank correlation. Using the studentised non-parametric bootstrap discussed by Jonathan & Ewans (2006), we have estimated bootstrap 95% confidence intervals for the parameters $\{A_{abk}\}_{a=1,b=1,k=0}^{2,2,p}$, γ and σ. In this approach to bootstrapping, we are careful to preserve the dependency structure between locations; data for all locations for any given storm is treated as a single multivariate observation for resampling. Bootstrap 95% intervals for the A_{abk}, assuming first order models for each of γ and σ, based on 500 storm-wise resamples of the H_S^{SP} data are given in Table 1. Corresponding bootstrap 95% intervals for γ and σ are shown in Figure 5.

Table 1: Point and interval estimates for first-order model parameters

Parameter	Estimate	Asymptotic 95%	Bootstrap 95%
A_{110}	-0.13	(-0.14,-0.13)	(-0.25,0.06)
A_{111}	0.24	(0.23,0.25)	(0.10,0.48)
A_{121}	0.24	(0.24,0.25)	(0.09,0.44)
A_{210}	1.97	(1.95,1.98)	(1.59,2.30)
A_{211}	-1.04	(-1.05,-1.02)	(-1.76,-0.60)
A_{221}	0.14	(0.12,0.15)	(-0.31,0.62)

Some technical details of the bootstrapping analysis need to be noted. For each of the 500 bootstrap resamples, a likelihood ratio test was performed to check that the first-order model (for both of γ and σ) could be justified over the corresponding constant model. Specifically, twice the difference of the negative log-likelihoods (known as "deviance") is compared with the critical value of the χ^2 distribution with 4 degrees of freedom (since the first order model has 4 more parameters that the constant model). Approximately 20 resamples for which the first-order model was rejected were ignored for estimation of

asymptotics. Further, as can be seen from Figure 5, the value of γ approaches -0.5 for some storm peak directions, causing numerical difficulties (because of the requirement of $\gamma > -0.5$) for estimation of asymptotic variances. To overcome this difficulty, we replace the term in $(1+2\gamma)$ in the expressions for elements of the information matrix by 0.2 for all $\gamma < -0.4$. Initial checks suggest that this approximation is reasonable. Appendix B confirms that the approximation provides interval estimates with reasonable coverage probabilities.

From the table and the figure it can be seen that asymptotic statistics greatly underestimate the uncertainties of parameters. Bootstrapping provides more realistic interval estimates. The bootstrap 95% interval for γ is always positive for some storm peak directions, and always negative for others, demonstrating the presence of directionally-dependent extremes.

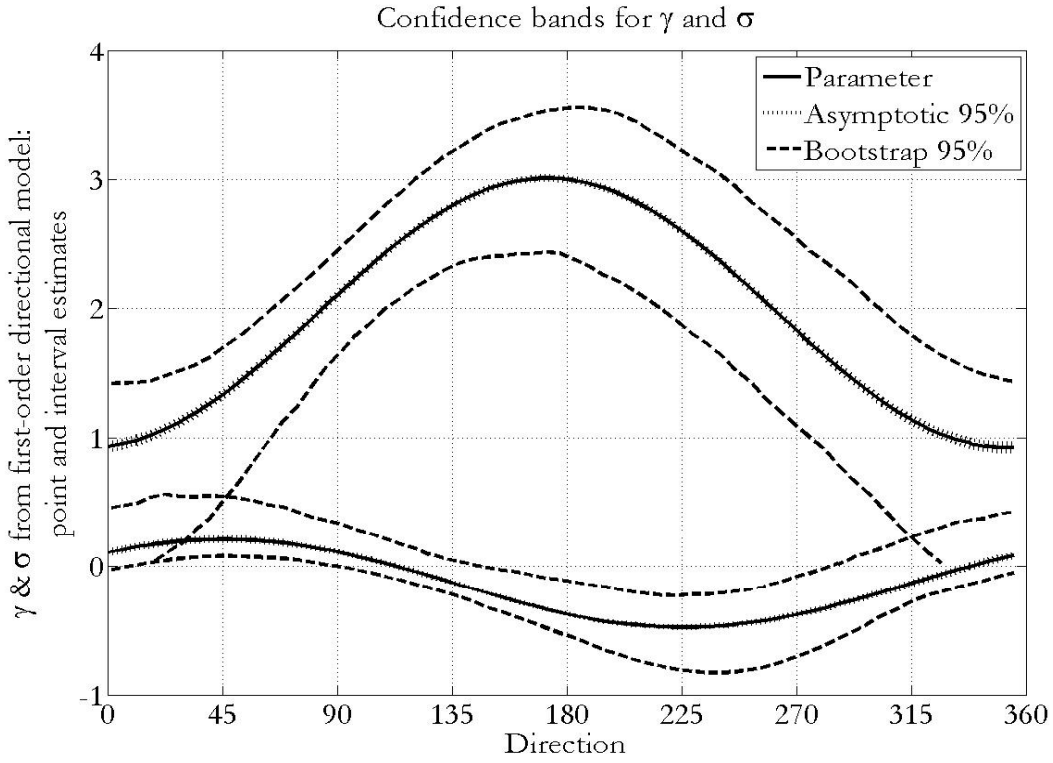

Figure 5. Point and interval estimates for γ and σ with storm peak direction.

4. ESTIMATION OF OMNI-DIRECTIONAL EXTREMES

We assume that, given any storm peak direction, θ_i, values of storm peak H_S above threshold u follow a GPD distribution with parameters $\gamma(\theta_i)$ and $\sigma(\theta_i)$ as introduced in section 3 above. We assume that the

occurrences of storms are independent Poisson events with expectation $\frac{1}{P_0}$ per annum per storm, where P_0 is the period of hindcast data. We further assume that the empirical distribution of storm peak directions given by the set $\{\theta_i\}_{i=1}^{n}$ provides an adequate representation of the distribution of storm peak directions for any period P of interest; that is, storm peak directions for any P are restricted to the set $\{\theta_i\}_{i=1}^{n}$. Robinson and Tawn (1997) and Chavez-Demoulin and Davison (2005) present a series of models of varying complexity appropriate for the current situation also.

Using the directional model introduced above, we now set out to estimate the cumulative distribution function of the maximum storm H_S for an arbitrary directional sector S, in the peak over threshold sense, corresponding to some period P of time. To achieve this, we consider the influence of storm events, the storm peak directions of which correspond to the sector S. However, we also must consider the influence of all other storm events on the sector, even though their storm peak directions fall outside S, since these storms may also include 30-minute sea states, the wave directions of which correspond to S. This effect is illustrated in Figure 6, which shows H_S versus wave direction for consecutive 30-minute sea states of a typical storm at a typical location.

From Figure 6, we see that H_S^{sp} corresponds to a wave direction of approximately 140º, but that sea states extend over a wide range of wave directions. Suppose now that we are interested in establishing design criteria for the first directional quadrant $[0,90)$. We quantify the contribution of the storm to sector $[0,90)$ in terms of the maximum value of sea state H_S (expressed as a fraction of H_S^{sp}) for any sea state whose wave direction falls within the sector. In general, we refer to this quantity as the directional influence $\rho_i(S)$ of storm event E_i $i=1,2,...,n$ on sector S. Thus, for the storm in Figure 6, the directional influence of the storm on sector $[0,90)$ is approximately 0.18. Similarly, the directional influence of the storm on quadrant $[90,180)$ is unity (since storm peak direction corresponds to this sector). The directional influence of the storm on quadrant $[270,360)$ is zero, since no sea states of the storm fall in this sector.

Directional influence therefore quantifies the maximum contribution of a storm to a directional sector as a fraction of storm peak H_S. From the GOMOS data, we can extract values for directional influence to facilitate estimation of maximum storm H_S for any storm-sector combination of interest. We characterise the extremal behaviour of X_i, the value of H_S^{sp} for any storm event E_i, given its storm peak direction, using the directional model from above, where X_i is GPD-distributed. The contribution of this storm event to any directional sector S is quantified in terms of the random variable $\rho_i(S)X_i$, namely the maximum contribution of the storm to the sector observed in the 105 years of GOMOS data. Since the storm events

$\{E_i\}_{i=1}^{n}$ are statistically independent, we can proceed to calculate the statistical properties of the maximum storm H_S in an arbitrary sector S as follows.

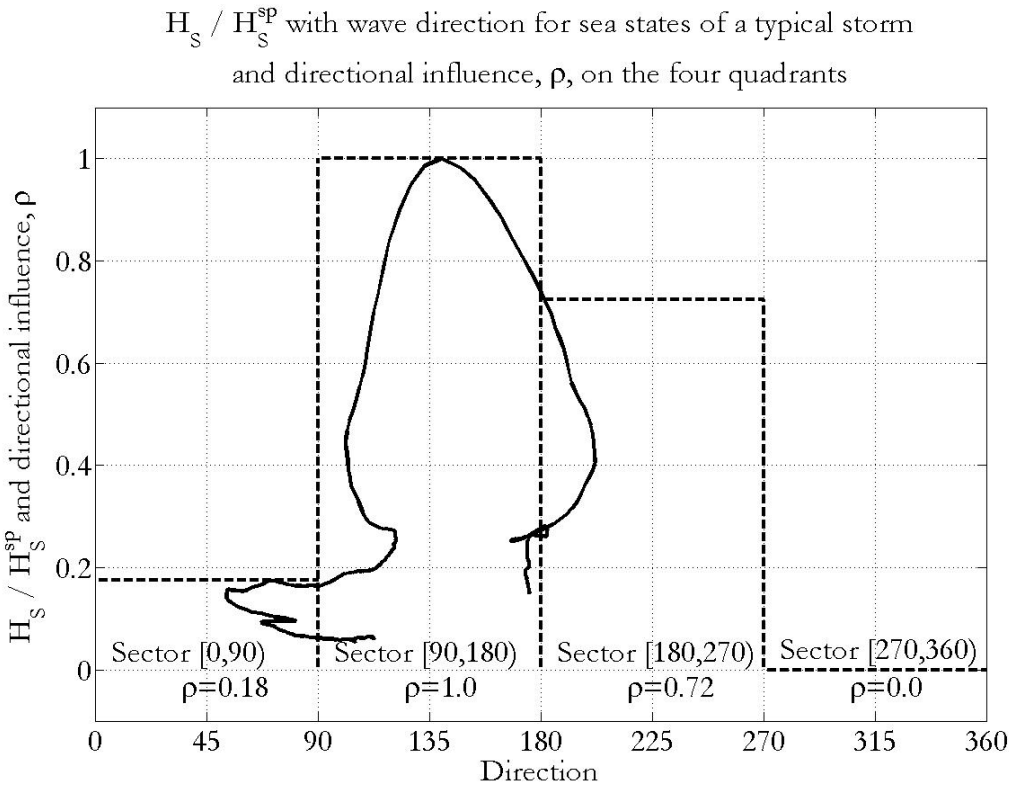

Figure 6: Variation of H_S/H_S^{sp} with wave direction (solid) for 30-minute sea states of a typical storm. H_S^{sp} corresponds to a storm peak direction of approximately 140°, but sea states extend over a wide range of wave directions. Also shown (dashed) is the directional influence of the storm on each of the four quadrants.

In any period P, the cumulative distribution function of the maximum storm H_S in sector S is given by $F_{X\max S}$:

$$F_{X\max S}(x) = P\left(X_{\max S} \le x \mid X_i > u \forall i, i \in [1,2,\ldots,n]\right) = \prod_{i=1}^{n}\left\{\sum_{k=0}^{\infty} P\left(\rho_i(S)X_i \le x \mid X_i > u, M_i = k\right)P\left(M_i = k\right)\right\}$$

where M_i is the number of occurrences of storm i in the period, the expected value of which is $m = \frac{P}{P_0}$ for all storms. Recalling that M_i is Poisson distributed, we have:

$$F_{X\max S}(x) = \prod_{i=1}^{n}\left\{\sum_{k=0}^{\infty}\left(1-\left(1+\frac{\gamma(\theta_i)}{\sigma(\theta_i)}\left(\frac{x}{\rho_i(S)}-u\right)\right)^{-\frac{1}{\gamma(\theta_i)}}\right)^{k}\frac{e^{-m}m^{k}}{k!}\right\}$$

$$= \prod_{i=1}^{n}\left\{\exp\left\{-m\left(1+\frac{\gamma(\theta_i)}{\sigma(\theta_i)}\left(\frac{x}{\rho_i(S)}-u\right)\right)^{-\frac{1}{\gamma(\theta_i)}}\right\}\right\}$$

$$= \exp\left\{-m\sum_{i=1}^{n}\left(1+\frac{\gamma(\theta_i)}{\sigma(\theta_i)}\left(\frac{x}{\rho_i(S)}-u\right)\right)^{-\frac{1}{\gamma(\theta_i)}}\right\}$$

Note, in particular, that if this sector was actually homogeneous so that $\gamma(\theta_i)=\gamma_S$, $\sigma(\theta_i)=\sigma_S$, and further if $\rho_i(S)=1 \quad \forall i$ then this expression would reduce to the standard GEV $\exp\left\{-mn_S\left(1+\frac{\gamma_S}{\sigma_S}(x-u)\right)^{-\frac{1}{\gamma S}}\right\}$, where mn_S is the expected number of storms in the sector in period P , n_S being the number of storms in S in P_0 (see, e.g. Coles and Walshaw (1994)). Leadbetter et al (1983) give the theoretical framework within which modelling maxima using GEV are valid."

Once the values of $\{\gamma(\theta_i),\sigma(\theta_i)\}_{i=1}^{n}$ have been estimated, the distribution of H_{S100}, the $P=100$ year maximum, can be estimated by setting the expression for $F_{X\max S}(x)=q$ for any quantile q, $q\in[0,1]$, and setting P = 100 years, then solving for x for an arbitrary sector. The most probable value H_{S100MP} of H_{S100} can be estimated by setting the second derivative of $F_{X\max S}(x)$ to zero and solving for x.

We can calculate sector maxima cumulants for the four quadrants ($[0,90)$, $[90,180)$, $[180,270)$ and $[270,360)$) and for the omni-directional (i.e. for sector $[0,360)$) for the GOMOS data. The resulting cumulative distribution functions for H_{S100} are given in Figure 7 for the directional model (using first-order models for each of γ and σ). As would be expected, given that we have observed that directional effects are important for extreme storm behaviour for these data, there are considerable differences between sector cumulants. Sectors $[0,90)$ and $[90,180)$ show much longer, heavier tails.

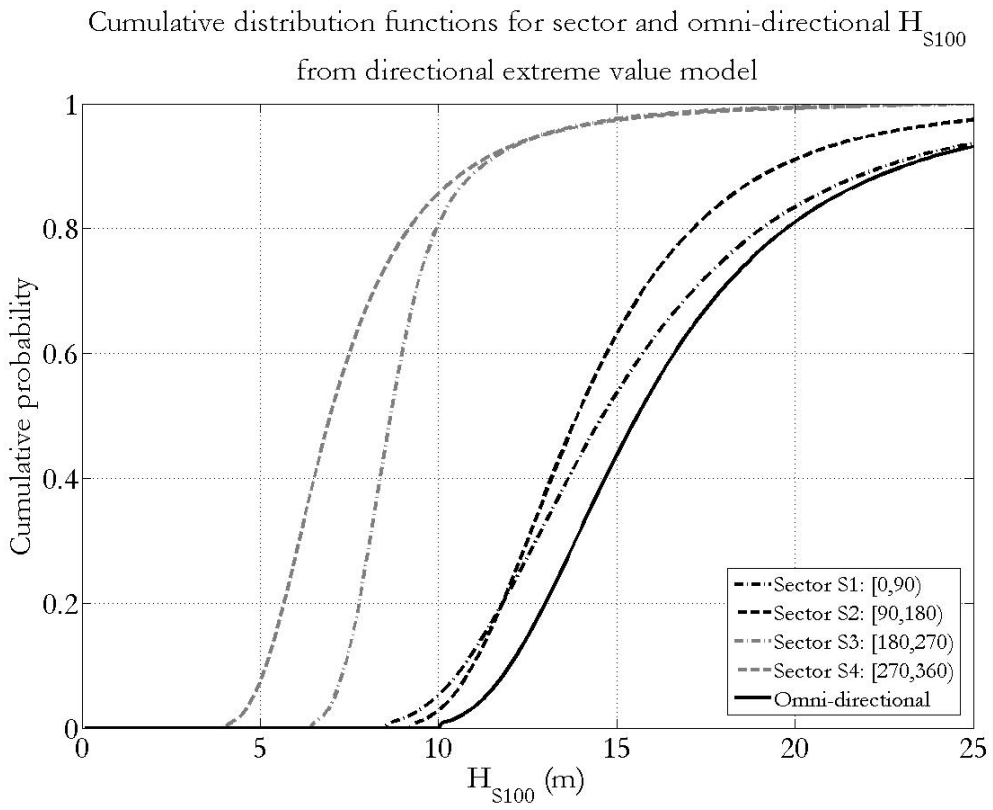

Figure 7: Cumulative distribution functions for sector and omni-directional H_{S100} for GOMOS, using a first-order directional model for each of extreme value shape and scale.

For comparison, we also give the corresponding cumulants (Figure 8) based on the direction-independent EV models (assuming γ and σ constant and independent of storm peak direction). Cumulants based on the directional EV model more accurately describe the data, notwithstanding the uncertainties in EV model parameters already discussed. In particular we note that the omni-directional cumulant based on the directional model has a longer and heavier right hand tail, indicating that large values of H_{S100} are more likely than we might anticipate were we to base our beliefs on EV models which ignore directionality.

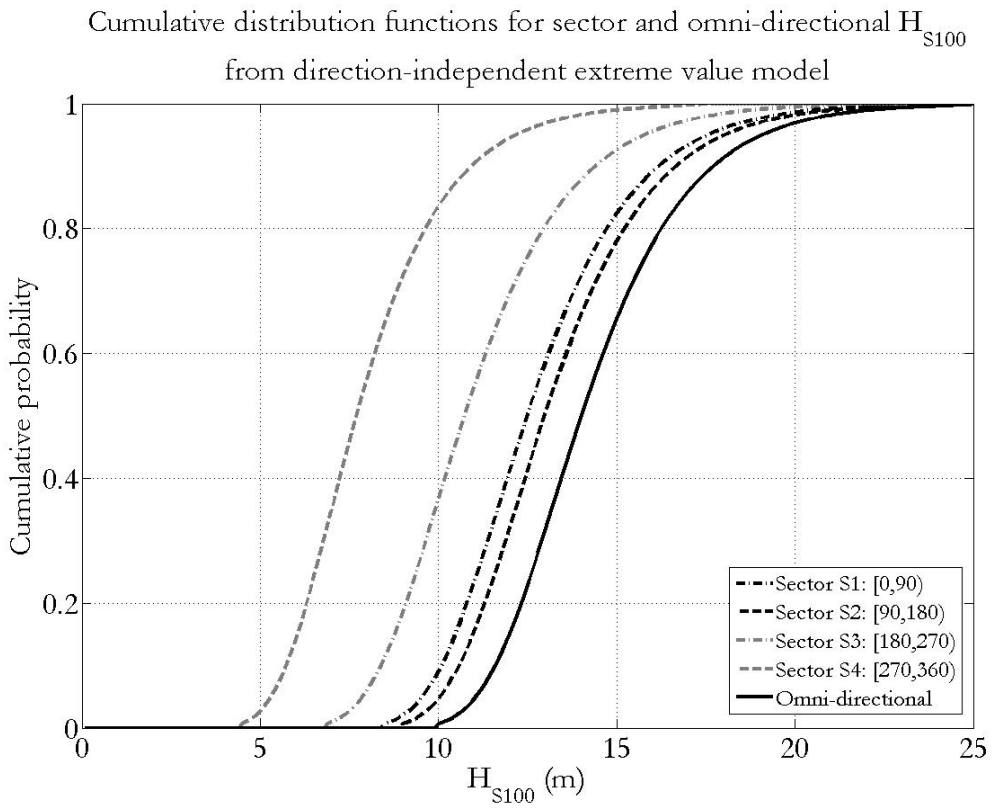

Figure 8: Cumulative distribution functions for sector and omni-directional H_{S100} for GOMOS, using a directional-independent model for each of extreme value shape and scale. The omni-directional cumulant in particular is lighter tailed than the correspond cumulant in Figure 7.

5. DESIGN CRITERIA FROM DIRECTIONAL EXTREMES

In this section, we consider the specification of design criteria for directional extremes. First, we introduce three different approaches to directional design, all consistent with the same given omni-directional design criterion, and discuss their relative characteristics. We introduce a simple 2-sector application for illustrative purposes. Then we propose a risk-cost optimisation criterion to aid the selection of a balanced set of directional design criteria, accommodating both design risk and cost. The characteristics of the risk-cost optimised design are illustrated for the 2-sector problem. Then we calculate directional design criterion for the GOMOS location using each of the three directional design approaches, for both the directional and direction-independent extreme value models discussed earlier.

Suppose we have a location at which occurrences of extremes storms can be partitioned with respect to direction into m directional sectors. Within each directional sector, extremes exhibit identical behaviour. But the extreme value characteristics of the sectors are different. We wish to establish appropriate design criteria for each sector consistent with a given omni-directional non-exceedence probability $q_{100Omni}$ at the 100-year return level.

Now consider the cumulative probability function $P\left(X_{\max 100Omni} \le x\right)$ for the maximum observed during the 100-year period in any sector $X_{\max 100Omni}$. Considering only the storm peak sea states, then

$$P\left(X_{\max 100Omni} \le x\right) = \prod_{i=1}^{m} P\left(X_{\max 100S_i} \le x\right)$$

where $P\left(X_{\max 100S_j} \le x\right)$ is the cumulative probability function for the maximum observed in the sectors $\{S_i\}_{i=1}^{m}$ in a 100 year period.

If design criteria are specified in terms of an omni-directional non-exceedence probability $q_{100Omni}$, we can immediately calculate the corresponding 100 year design H_S by inverting the equation $q_{100Omni} = P\left(X_{\max 100Omni} \le x_{100Omni}\right)$ to obtain $x_{100Omni}$. However, specification of $q_{100Omni}$ does not allow us to determine unique values for sector design H_S. All that the omni-directional specification does is impose the constraint $q_{100Omni} = \prod_{i=1}^{m} q_{100S_i}$, where q_{100S_i} are non-exceedence probabilities for the sectors $\{S_i\}_{i=1}^{m}$. That is, the product of sector non-exceedence probabilities must equal the omni-directional equivalent. This constraint leaves us free to specify any set of sector design H_S values $\left\{x_{100S_i}\right\}_{i=1}^{m}$ such that $q_{100S_i} = P\left(X_{\max 100S_i} \le x_{100S_i}\right) \quad \forall i$ and $q_{100Omni} = \prod_{i=1}^{m} q_{100S_i}$. An infinite number of solutions exist, but it is instructive to consider a number of interesting cases.

(1) Suppose that all sectors but one exhibited extreme value behaviour with negative tail index, γ. For each of these sectors, an upper limit for the value of storm peak H_S therefore exists. It would therefore be possible to set the sector design values for all these sectors to their maximum value. The corresponding non-exceedence probabilities would all be unity. Then, $q_{100Omni} = \prod_{i=1}^{m} q_{100S_i} = q_{100S^*}$, were S^* is the remaining sector with positive index. In this case, the omni-directional non-exceedence probability would correspond to that of the most extreme sector.

(2) Another choice would be to design all sectors to the omni-directional design H_S, $x_{100Omni}$. Since $P\left(X_{\max 100Omni} \le x\right) = \prod_{i=1}^{m} P\left(X_{\max 100S_i} \le x\right)$ for any value of x, and for $x_{100Omni}$ in particular, we set $q_{100S_i} = P\left(X_{\max 100S_i} \le x_{100Omni}\right) \quad \forall i$ thereby ensuring that $q_{100Omni} = \prod_{i=1}^{m} q_{100S_i}$ is satisfied. We refer to this design as the "omni-directional H_{S100} " design. Figure 9 illustrates this method of selection of

sector design criteria in the case $m = 2$ for ease of discussion. In this example, sector S1 is more severe that sector S2. Naturally, the sector design non-exceedence probabilities are both larger than the omni-directional value, but we note that the non-exceedence probability for the more severe sector (S1) is less than that for the less severe sector (S2). It is clear in general that sector non-exceedence probabilities $\left\{q_{100S_i}\right\}_{i=1}^{m}$ will be very different to each other. Indeed, the non-exceedence probabilities for the most severe sectors will always be lower that those for less severe sectors. But even for the most severe sector, sector non-exceedence probability will always be at least as large as the omni-directional value.

(3) A third possibility is to maximise the value of the minimum sector non-exceedence probability. This is achieved by setting the same non-exceedence probability for each sector. In this case we have $q_{100Omni} = \prod_{i=1}^{m} q_{100S} = \left(q_{100S}\right)^m$ where $q_{100S} = \left(q_{100Omni}\right)^{\frac{1}{m}}$ is the common sector non-exceedence probability. We refer to this design as the "equal sector non-exceedence" design. Figure 10 illustrates the approach in the case $m = 2$. Now we impose more demanding non-exceedence requirements equally across all sectors, including the most severe. Note that, for any homogeneous sample size n corresponding to time period P_o years, from a generalised Pareto distribution with parameters γ and σ, we have $\frac{nP}{P_O}\left(1+\frac{\gamma}{\sigma}(x-u)\right)^{-\frac{1}{\gamma}} = -\ln q$ which defines the relationship between the P year non-exceedence probability q and extreme quantile x. Setting the extreme 100 year quantile using a non-exceedence probability $q^{\frac{1}{m}}$ (so that

$\frac{100n}{P_O}\left(1+\frac{\gamma}{\sigma}(x-u)\right)^{-\frac{1}{\gamma}} = -\ln q^{\frac{1}{m}} = -\frac{1}{m}\ln q$) is equivalent to a non-exceedence probability q at the $100m$-year level. Thus, this approach sets $100m$-year return levels for each directional sector. Specifically, in the case $m = 8$ we would set 800-year return levels in each sector.

We see that the particular choices of $\left\{x_{100S_i}\right\}_{i=1}^{m}$ discussed above are all valid, but have very different characteristics and design consequences. We might judge, if we were to follow the third approach above, that setting the most extreme sector at the $100m$-year level was over-conservative. At the same time, we might like to introduce more conservatism for the most severe sector than that produced by the second approach above. For this reason, we might consider a risk-cost basis for optimisation of directional design criteria. If $c(x)$ is the cost of designing to a storm peak H_S of x metres, then the overall cost of design will be $RC = \sum_{i=1}^{m} c\left(x_{100S_i}\right)$, where $x_{100S_i} = x_{100S_i}\left(q_{100S_i}\right)$ is the sector storm peak H_S corresponding to sector non-exceedence probability q_{100S_i}. The optimal design is that which mimises RC subject to

$q_{100Omni} = \prod_{i=1}^{m} q_{100S_i}$ where $q_{100Omni}$ is some quantile (typically ≥ 0.5) of the omni-directional cumulative distribution.

For our two-sector problem, Figure 11 illustrates risk-cost optimisation. For simplicity, we assume that the cost of construction for either sector takes the form $c(x) = Kx^2$, for x in metres, where for convenience we set $c(10) = 1$, so that $K = 0.01$. We further set $q_{100Omni} = 0.5$. We see that optimal risk-cost design corresponds to minimum total design cost given $q_{100Omni} = 0.5$. The optimal risk-cost design (labelled "A") is a compromise between designing to the omni-directional H_S in all sectors (labelled "B"), and designing to equal non-exceedence probabilities in each sector (labelled "C").

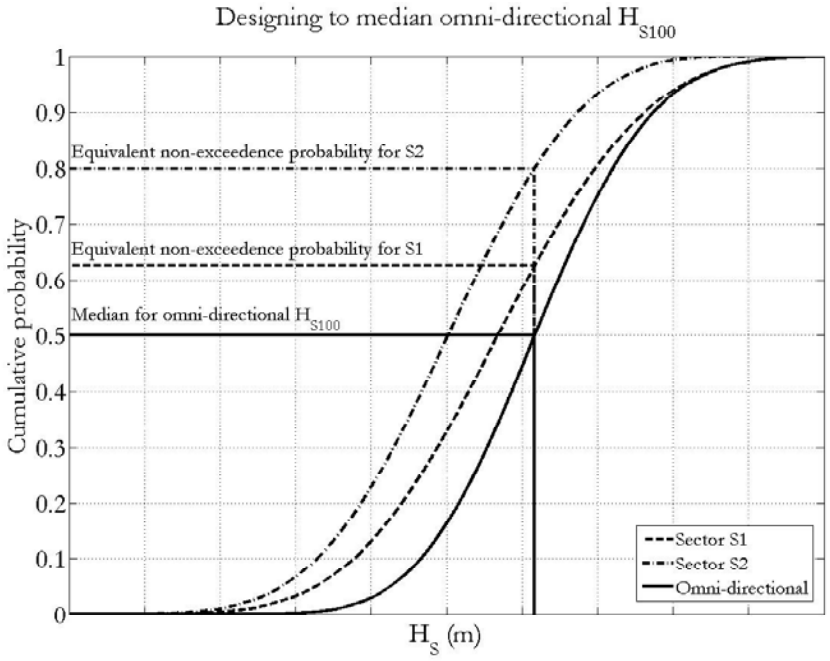

Figure 9: Designing to median omni-directional H_{S100}, for the two-sector problem. The equivalent sector non-exceedence probability is smaller for the more severe sector.

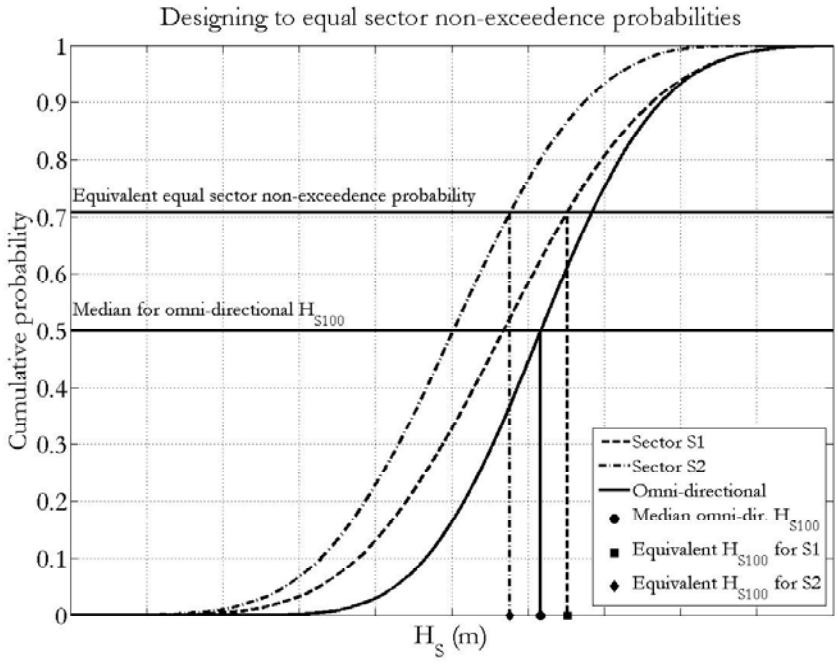

Figure 10: Designing to equal non-exceedence probabilities for each sector, illustrated for the two-sector problem. The equivalent sector H_S for the more severe sector is larger than the omni-directional value.

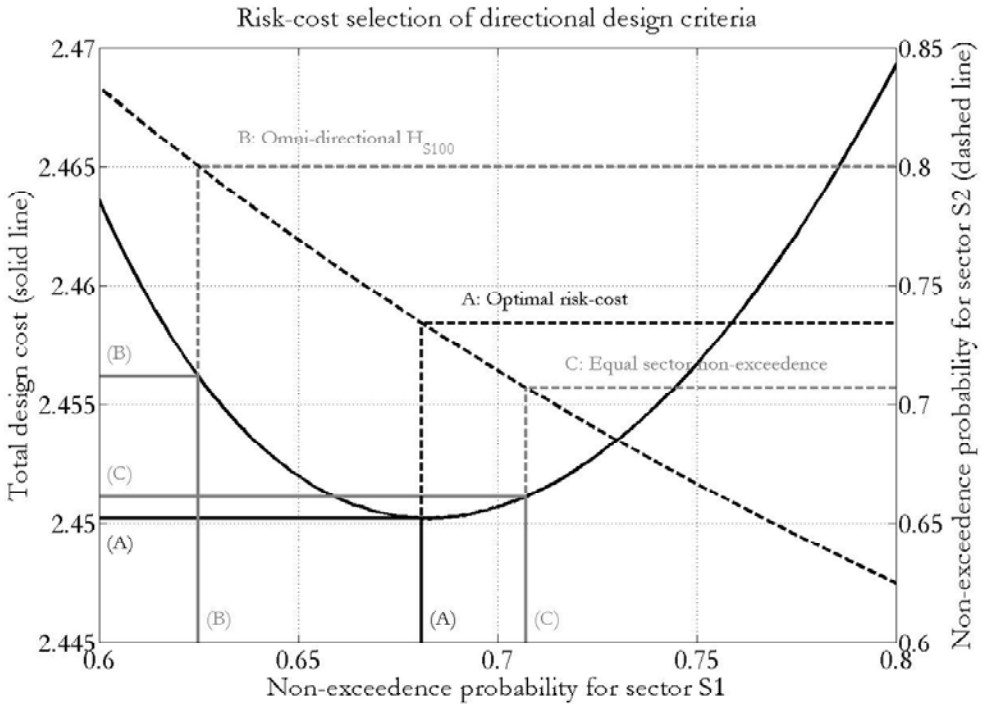

Figure 11: Directional design criteria optimising risk-cost for the two-sector problem. Shown, as a function of non-exceedence probability for sector S1, are: total design cost (solid line, with ordinate on left hand side) and corresponding non-exceedence probability for sector S2 (dashed line, with ordinate on right hand side). The optimal design (labelled "A") minimises total design cost for a risk level quantified in terms of a non-exceedence probability for H_{S100} of $q_{100Omni} = 0.5$. Also shown (in grey) are the "omni-directional H_{S100} " design (labelled "B") and the "equal sector non-exceedence" design (labelled "C").

Table 2: Design criteria based on median omni-directional H_{S100}

Sector	Angle	Risk-cost optimal			Omni-directional H_{S100}			Equal sector non-exceedence		
Directional model										
		RC	x_{100S_i}	q_{100S_i}	RC	x_{100S_i}	q_{100S_i}	RC	x_{100S_i}	q_{100S_i}
S1	[0,90)	8.78	18.03	0.75	9.73	15.60	0.59	9.29	20.20	0.84
S2	[90,180)		17.40	0.81		15.60	0.69		17.90	0.84
S3	[180,270)		11.44	0.91		15.60	0.98		10.30	0.84
S4	[270,360)		10.90	0.90		15.60	0.98		9.70	0.84
Direction-independent model										
		RC	x_{100S_i}	q_{100S_i}	RC	x_{100S_i}	q_{100S_i}	RC	x_{100S_i}	q_{100S_i}
S1	[0,90)	7.56	15.00	0.82	7.84	14.00	0.72	7.59	15.20	0.84
S2	[90,180)		15.40	0.82		14.00	0.66		15.70	0.84
S3	[180,270)		13.41	0.84		14.00	0.88		13.40	0.84
S4	[270,360)		10.67	0.89		14.00	0.98		10.10	0.84

Table 2 and Table 3 present design criteria from the GOMOS data set, for design to non-exceedence probabilities of 0.5 and 0.7 for omni-directional H_{S100}, based on three design approaches and two extreme value models. The corresponding values for an annual probability of exceedance of 0.01 are given in Appendix B. Looking at Table 2 first, comparing the top and bottom halves of the table, we see that design values based on the directional model are larger that their counterparts obtained by ignoring the directional dependence of storms. This indicates that ignoring directionality results in underestimation of extreme storm behaviour. Results also illustrate the different characteristics of the three design approaches used. The risk-cost optimal design avoids the more extreme properties of the other design methods, such as the large range of values for $\left\{q_{100S_1}\right\}_{i=1}^{m}$ present for design to omni-directional H_{S100}, and the large range of values for $\left\{x_{100S_1}\right\}_{i=1}^{m}$ evident for design to equal sector non-exceedences. Taking the risk-cost optimal

design based on the directional EV model to be most preferrable, we conclude that we need to design for 18m in sector S1, 17.4m in S2, but only 11.4m and 10.9m respectively in sectors S3 and S4.

Table 3: Design criteria based on omni-directional H_{S100} non-exceedence of 0.7

Sector	Angle	Risk-cost optimal			Omni-directional H_{S100}			Equal sector non-exceedence		
Directional model										
		RC	x_{100S_i}	q_{100S_i}	RC	x_{100S_i}	q_{100S_i}	RC	x_{100S_i}	q_{100S_i}
S1	[0,90)	11.55	20.97	0.86	12.82	17.90	0.74	12.20	23.40	0.92
S2	[90,180)		19.67	0.90		17.90	0.84		20.20	0.92
S3	[180,270)		12.92	0.95		17.90	0.99		11.60	0.92
S4	[270,360)		12.70	0.95		17.90	0.99		11.40	0.91
Direction-independent model										
		RC	x_{100S_i}	q_{100S_i}	RC	x_{100S_i}	q_{100S_i}	RC	x_{100S_i}	q_{100S_i}
S1	[0,90)	8.99	16.30	0.91	9.36	15.30	0.85	9.03	16.50	0.91
S2	[90,180)		16.70	0.90		15.30	0.81		17.00	0.92
S3	[180,270)		14.70	0.91		15.30	0.94		14.70	0.91
S4	[270,360)		11.76	0.94		15.30	0.99		11.20	0.91

In addition to reflecting the trends of the previous table, Table 3 quantifies the extent to which basing design on H_{S100} non-exceedence probability of 0.7 increases design values for all models and design methods, and for the chosen risk-cost optimal design based on the directional EV model in particular.

6. CONCLUSIONS AND RECOMMENDATIONS

Directional metocean data allow the possibility for directionality to be taken into account in the design of offshore structures, but care must be taken to ensure that models and design criteria are developed and applied consistently.

A directional extremes model (a Fourier series expansion here) allows directionally consistent extreme values to be developed, with obvious applicability for engineering design. There is a strong general case in favour of adopting a directional extreme value model to storm peak H_S data unless it can be demonstrated statistically that a direction-free model is no less appropriate. For the current GOMOS hindcast sample, a directional GPD model explains the data significantly better than the conventional (direction-free) model. A first-order Fourier series model was found adequate for the GOMOS data analysed, but we expect that higher order models would be necessary for locations with more complex directionality.

It is important to consider the directionality of sea states when developing extremal criteria. Omni-directional extreme values derived from a directional model can be significantly different from a direction-independent derivation, which ignores the distribution variability of the data with direction. For example, when the directional dependence of the GOMOS data is modeled with a Fourier series expansion, the omni-directional H_{S100} is heavier tailed than that derived from a direction-independent approach, indicating that large values of H_{S100} are more likely than we might anticipate were we to base our beliefs on EV models which ignore directionality.

In this work, we model extremal properties of storm peak H_S as a function of wave direction at storm peak, in the peak over threshold sense, taking each storm event to be independent statistically for a given location. We therefore ignore all but the most severe 30-minute sea state of the storm for extreme value analysis. In estimating maximum storm H_S for a directional sector, we accommodate the effects of all sea states of all storms whose wave directions fall within that directional sector, regardless of the wave direction at storm peak, by quantifying the directional influence of storms on the directional sector directly from the GOMOS data.

The rate of occurrence of storms peaks is dependent on storm peak direction in general. Hence the distribution of H_{S100} will have storm peak directional dependence in general, even when the extremal value characteristics (e.g GPD shape and scale) of storm peak H_S are independent of storm peak direction. The evidence from the current GOMOS data is that the rate of occurrence of storms shows strong storm peak directional dependence.

The process of setting criteria for a number of directional sectors for a given omni-directional non-exceedance probability is not unique. Nevertheless, directional design criteria provide more specific estimates of extreme offshore conditions enabling the risk associated with a design to be minimised given available resources. We propose a risk-cost basis as an objective method for optimizing directional criteria, while preserving overall reliability. The risk-cost optimal design avoids more extreme properties of the other design methods, such as the large range of values of sector non-exceedance probabilities in the design to omni-directional value, or the large range of sector extremes in the design to equal sector non-

exceedances.

ACKNOWLEDGEMENTS

The authors acknowledge the support of Shell International Exploration and Production and Shell Research Limited for this work. The authors further acknowledge useful discussions with George Forristall and Michael Vogel, and the assistance of Joost den Haan in data handling and computing support.

APPENDIX A: MAXIMUM LIKELIHOOD ESTIMATION OF PARAMETERS FOR DIRECTIONAL MODEL

The negative log likelihood l is given by:

$l = \sum_{i=1}^{n} l_i$, where $l_i = \log\sigma_i + \left(\frac{1}{\gamma_i} + 1\right)\log\left(1 + \frac{\gamma_i}{\sigma_i}(X_i - u)\right)$, and $\gamma_i = \gamma(\theta_i)$, $\sigma_i = \sigma(\theta_i)$, $i = 1, 2, \ldots, n$ .Thus:

$$\frac{\partial l_i}{\partial \gamma_i} = -\frac{1}{\gamma_i^2}\left(\log G_i - (1+\gamma_i)\left(1 - \frac{1}{G_i}\right)\right) \text{ where } G_i = 1 + \frac{\gamma_i}{\sigma_i}(X_i - u)$$

$$\frac{\partial l_i}{\partial \sigma_i} = -\frac{1}{\gamma_i\sigma_i} + \frac{1}{\sigma_i}\left(1 + \frac{1}{\gamma_i}\right)\frac{1}{G_i}$$

Using the chain rule for partial differentiation, we have:

$\frac{\partial l}{\partial A_{abk}} = \sum_{i=1}^{n} U_{ai} t_b(k\theta_i)$, $a = 1,2$, $b = 1,2$, $k = 0, 1, \ldots, p$ where $U_{ai} = \frac{\partial l_i}{\partial \gamma}$ for $a = 1$, and $\frac{\partial l_i}{\partial \sigma}$ for $a = 2$, recalling that $A_{a20} \triangleq 0$ Maximum likelihood estimates are obtained by setting $\frac{\partial l}{\partial A_{abk}} = 0$ $\forall a, b, k$ and solving.

Second derivatives of the likelihood can be found in a similar fashion. First, expressions for $\left\{\frac{\partial^2 l}{\partial A_{abk}\partial A_{\alpha\beta\kappa}}\right\}$ $\forall a, b, k, \alpha, \beta, \kappa$ are found by applying the chain rule to the expressions above. Then expectations are taken. Using the identities $E_X\left[\left(1 + \frac{\gamma}{\sigma}(X-u)\right)^{-r}\right] = \frac{1}{1+\gamma r}$ for $1 + \gamma r > 0$, (which can be evaluated directly using $E_X(g(X)) = \int g(x) f_X(x)\, dx$) and $E_X\left[\left(\log\left(1 + \frac{\gamma}{\sigma}(X-u)\right)\right)^r\right] = (-\gamma)^r \Gamma(r+1)$ for integer r , (which can be evaluated directly, noting e.g. the similarity the integrand with the density of the gamma random variable), when $X \sim GPD(\gamma, \sigma)$, these expressions reduce to the form:

$$E_X\left[\frac{\partial^2 l}{\partial A_{abk}\partial A_{\alpha\beta\kappa}}\right] = \sum_{i=1}^{n} \frac{B_{a\alpha i}}{C_i} t_b(k\theta_i) t_\beta(\kappa\theta_i) \quad \forall a, b, k, \alpha, \beta, \kappa$$

where $B_{a\alpha i} = \begin{Bmatrix} 2\sigma^2(\theta_i),\ a=\alpha=1 \\ (1+\gamma(\theta_i)),\ a=2,\alpha=1 \\ \sigma(\theta_i),\ a=\alpha=2 \end{Bmatrix}$

and $C_i = \sigma^2(\theta_i)(1+\gamma(\theta_i))(1+2\gamma(\theta_i)) \quad \forall i$

The asymptotic variances for parameter estimates can be read from the asymptotic covariance matrix for parameter estimates, given by the inverse I^{-1} of the information matrix $I = E_X\left[\left\{\frac{\partial^2 l}{\partial A_{abk}\partial A_{\alpha\beta\kappa}}\right\}\right]$.

Moreover, the asymptotic variance of a function $g(\{A_{abk}\})$ of the parameters is given by $var_A\left(g(\{A_{abk}\})\right) = \left[\frac{\partial g}{\partial A_{abk}}\right]' I^{-1}\left[\frac{\partial g}{\partial A_{abk}}\right]$ where $\left[\frac{\partial g}{\partial A_{abk}}\right]$ represents a vector with elements $\left\{\frac{\partial g}{\partial A_{abk}}\right\}$.

APPENDIX B. COVERAGE PERFORMANCE OF BOOTSTRAP INTERVAL ESTIMATES FOR PARAMETERS OF CYCLIC MODEL

The coverage performance of bootstrap interval estimates for the parameters of the first order cyclic models for extreme value shape and scale parameters was evaluated for three different cases (Independent (I), Dependent (D) and Resample (R)), when the true data model is known. The main motivation of the study was to ensure that bootstrap interval estimates are realistic for different spatial dependency between locations.

We performed the following simulation study. Data samples of size 315 storms for 120 locations were generated using the first order cyclic model (for each of extreme value shape and scale) with parameters estimated using the true GOMOS data (and given in Table 1) for each location, for three different situations. In the first case (Independent), independent data samples were generated for each location. In the second case, (Dependent), identical data were used for each location for any given storm. In the third case, (Resample), a resample (storm-wise across all locations) of the actual GOMOS data was used. The Independent and Dependent cases correspond to limiting dependence structures that we would encounter in practice.

For at least 1000 realisations of the data, 200 bootstrap samples were used to estimate extreme value parameter uncertainty. Results are given in Figure B 1 below, in terms of fraction of realisations for which the real parameter values of the first order cyclic model fall outside of the bootstrap interval estimate on the left and right hand sides. (The actual number of realisations used for each of Independent, Dependent and Resample studies was 1000, 1700 and 1500 respectively due to different computational requirements and

computing resources available for the different simulations. This will be updated to a fixed number for each of Independent, Dependent and Resample in due course).

Table B 1: Low and high bootstrap confidence interval exceedance probabilities for the Independent (I), Dependent (D) and Resample (R) cases

Parameter	I:Low	I:High	D:Low	D:High	R:Low	R:High
A110	0.09	0.01	0.06	0.04	0.06	0.06
A111	0.05	0.02	0.06	0.04	0.04	0.12
A121	0.02	0.06	0.07	0.05	0.05	0.08
A210	0.01	0.10	0.04	0.05	0.06	0.03
A211	0.03	0.03	0.05	0.05	0.13	0.02
A221	0.09	0.02	0.06	0.03	0.07	0.04

In the table, we expect total exceedance probability to be 0.05, since we are using a 95% interval, with 0.025 exceedance probabilities on each of the left-hand and right-hand sides. Values in Table B 1 confirm that the bootstrap confidence interval estimate is performing adequately in all three cases; numbers of exceedances are generally consistent with expectation. Figure B 1 and Figure B 2 illustrate low and high bootstrap confidence interval exceedance probabilities for extreme value shape and scale as a function of storm peak direction. Again, results are broadly consistent with expectation.

We conclude from these simulation studies that the bootstrap interval estimates for cyclic model parameters, and model parameter variability with storm peak direction, are realistic.

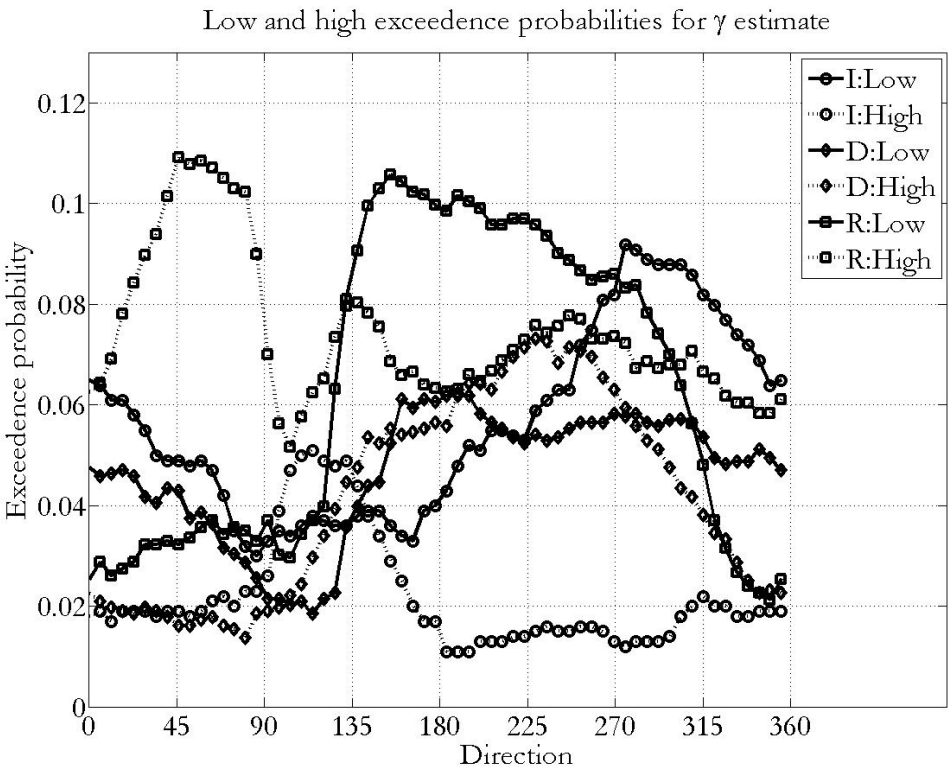

Figure B 1: Low and high bootstrap confidence interval exceedance probabilities of γ for the Independent (I), Dependent (D) and Resample (R) cases

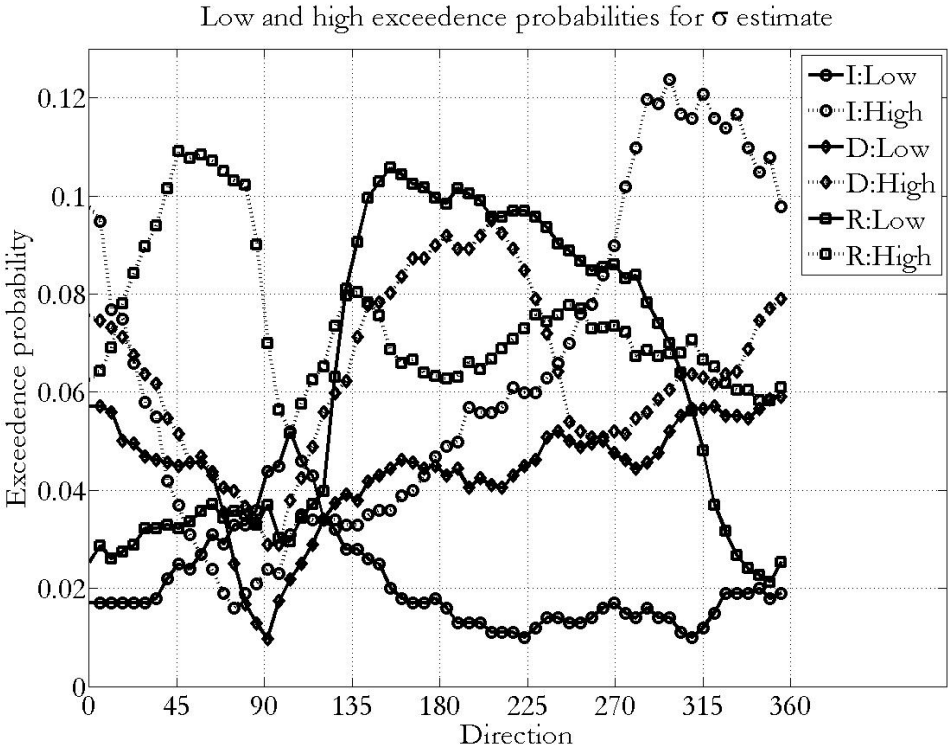

Figure B 2: Low and high bootstrap confidence interval exceedance probabilities of σ for the Independent (I), Dependent (D) and Resample (R) cases

Appendix C. Design criteria based on omni-directional H_{S100} non-exceedence of 0.37 (Annual probability of non-exceedance of 0.99)

Table C 1 Design criteria based on omni-directional H_{S100} non-exceedence of 0.37

Sector	Angle	Risk-cost optimal			Omni-directional H_{S100}			Equal sector non-exceedence		
Directional model										
		RC	x_{100S_i}	q_{100S_i}	RC	x_{100S_i}	q_{100S_i}	RC	x_{100S_i}	q_{100S_i}
S1	[0,90)	7.55	16.60	0.67	8.29	14.40	0.48	8.03	18.60	0.78
S2	[90,180)		16.20	0.74		14.40	0.56		16.80	0.78
S3	[180,270)		10.80	0.88		14.40	0.97		9.80	0.78
S4	[270,360)		10.04	0.86		14.40	0.97		8.90	0.78
Direction-independent model										
		RC	x_{100S_i}	q_{100S_i}	RC	x_{100S_i}	q_{100S_i}	RC	x_{100S_i}	q_{100S_i}
S1	[0,90)	6.83	14.29	0.76	7.08	13.30	0.63	6.85	14.50	0.78
S2	[90,180)		14.70	0.75		13.30	0.55		15.00	0. 78
S3	[180,270)		12.70	0.78		13.30	0.83		12.70	0. 78
S4	[270,360)		10.05	0.84		13.30	0.97		9.40	0. 78

REFERENCES

Casson E. and S. G. Coles 1999: Spatial regression models for extremes. *Extremes*, 1, p449.

Chavez-Demoulin, V. and A.C. Davison 2005: Generalized additive modelling of sample extremes. *Journal of the Royal Statistical Society. Series C: Applied Statistics* 54 (1), pp. 207-222

Coles S.G. and D. Walshaw 1994: Directional modelling of extreme wind speeds. *Applied Statistics*, 43, p139.

Coles S. G. and J. A. Tawn 1996: A Bayesian analysis of extreme rainfall data. *Applied Statistics*, 45, p463.

Coles S. G. and E. A. Powell 1996: Bayesian methods in extreme value modelling: a review and new developments. *International Statistics Review*, 64, p119.

Coles S. G. and E. Casson 1998: Extreme value modelling of hurricane wind speeds. *Structural Safety*, 20, p283.

Coles S. G. and J. A. Tawn 2005: Bayesian modelling of extreme sea surges on the UK east coast. *Phil.Trans.R.Soc. A*, 363, p1387.

Coles, S. and E. Simiu 2003: Estimating uncertainty in the extreme value analysis of data generated by a hurricane simulation model. *J Engineering Mechanics*, 129, 1288-1294.

Davison, A. C. and D. A. Hinkley 1997: *Bootstrap Methods and their Application*. Cambridge Series in Statistical and Probabilistic Mathematics, Cambridge University Press (Cambridge, UK).

Efron, B. and R. J. Tibshirani 1993: *An introduction to the bootstrap*. Chapman and Hall (New York).

Elsinghorst C., Groeneboom P., Jonathan P., Smulders L., and P.H. Taylor 1998: Extreme value analysis of North Sea storm severity. *J Offshore Mechanics Ocean Engineering*, 120, p177.

Forristall, G.Z., R.D. Larrabee, and R.S. Mercier 1991: Combined oceanographic criteria for deepwater structures in the Gulf of Mexico. *Offshore Technology Conference Proceedings*, OTC 6541, Houston.

Forristall, G.Z., 2004: On the use of directional wave criteria. *J. Wtrwy., Port, Coast., Oc. Eng.*, 130, p272.

Hall, P. 1988: *The bootstrap and Edgeworth expansion*. Springer Verlag (New York).

Heffernan, J. E. and J. A. Tawn 2004: A conditional approach for multivariate extreme values. *J R Statist Soc B*, 66, 497-546.

Jonathan, P. and K.C. Ewans 2006: Uncertainties in extreme wave height estimates for hurricane dominated regions. *Proceedings 25th International Conference on Offshore Mechanics and Arctic Engineering*, June 4-8, 2006, Hamburg, Germany.

Kotz S. and S. Nadarajah 2000: *Extreme Value Distributions: Theory and Applications*. Imperial College Press (London, UK).

Leadbetter, M. R., Lindgren, G. and H. Rootzen 1983: *Extremes and related properties of random sequences and series*. Springer (New York, USA).

Pickands, J. 1975: Statistical inference using extreme order statistics, *Ann Statist*, 3, p119.

Oceanweather Inc. 2005: GOMOS -- USA Gulf of Mexico Oceanographic Study, Northern Gulf of Mexico Archive, October, 2005.

Reiss R.D. and M. Thomas 2001: *Statistical analysis of extreme values*. Birkhauser Verlag (Basel, Switzerland).

Robinson, M. E. and J. A. Tawn 1997: Statistics for extreme sea currents. *Applied Statistics*, 46, p183.